

Folate dietary insufficiency and folic acid supplementation similarly impair metabolism and compromise hematopoiesis

Curtis J. Henry,^{1,2,3} Travis Nemkov,¹ Matias Casás-Selves,^{1,4} Ganna Bilousova,⁵ Vadym Zaberezhnyy,¹ Kelly C. Higa,² Natalie J. Serkova,⁷ Kirk C. Hansen,¹ Angelo D'Alessandro¹ and James DeGregori^{1,2,6,8*}

¹Department of Biochemistry and Molecular Genetics, University of Colorado AMC, Aurora, CO, USA; ²Department of Immunology and Microbiology, University of Colorado AMC, Aurora, CO, USA; ³Current address: Department of Pediatrics, Emory University, Atlanta, GA, USA; ⁴Current address: Ontario Institute for Cancer Research, Toronto, ON, Canada; ⁵Department of Dermatology and Charles C. Gates Center for Regenerative Medicine, University of Colorado AMC, Aurora, CO, USA; ⁶Department of Medicine, Section of Hematology, University of Colorado AMC, Aurora, CO, USA; ⁷Department of Anesthesiology, University of Colorado AMC, Aurora, CO, USA and ⁸Department of Pediatrics, Section of Hematology/Oncology, University of Colorado AMC, Aurora, CO, USA

©2017 Ferrata Storti Foundation. This is an open-access paper. doi:10.3324/haematol.2017.171074

Received: April 18, 2017.

Accepted: September 6, 2017.

Pre-published: September 7, 2017.

Correspondence: james.degregori@ucdenver.edu

Supplemental Methods

Folic Acid Detection

Mice were maintained on CD, FD, and SD diets as described above. Folic acid levels in the serum from mice maintained on various folate diets were determined per the manufacturer's instructions (ALPCO Folic Acid Vitamin B9 Microbiological Test Kit; Catalog No. 30-KIF005). Turbidity was determined using the Promega Glomax Multi + Detection System ELISA plate reader at 610-630 nm. The turbidity is directly proportional to the folic acid-dependent growth of *Lactobacillus rhamnosus* over the 48 hour incubation period.

Mass Spectrometry Analysis for Organ Metabolomics

Sample Preparation: Bone marrow B-cell progenitors were isolated by anti-B220 Magnetic Activated Cell Sorting (to >95% B220⁺) (Miltenyi Biotec), counted, pelleted at 1500 g for 10 min at 4°C, and stored at -80°C until analysis. Other tissues were snap frozen as small pieces in liquid nitrogen. Prior to UHPLC-MS analysis, samples were placed on ice and re-suspended with methanol:acetonitrile:water (5:3:2, v:v) at a concentration of 2 million cells per ml. For other organs, sample input was normalized by tissue weight and extracted at a concentration of 10 mg/mL. Suspensions were vortexed continuously for 30 min at 4°C. Insoluble material was removed by centrifugation at 10,000 g for 10 min at 4°C and supernatants were isolated for metabolomics analysis by UHPLC-MS.

UHPLC-MS analysis: Ten µl of cell extracts were injected into an UHPLC system (Ultimate 3000, Thermo, San Jose, CA, USA) and separated on a Kinetex C18 column (150x2.1 mm i.d., 1.7 µm particle size – Phenomenex, Torrance, CA, USA) using a 3 minute isocratic gradient at 250 µl/min (mobile phase: 5% acetonitrile, 95% 18 mΩ H₂O, 0.1% formic acid) or a BEH Amide column (150x2.1 mm i.d., 1.8 µm particle

size – Waters Corporation, Milford, MA, USA) at 350 μ l/min using (A) 95% acetonitrile, 10 mM ammonium acetate, pH 10.2 and (B) 5% acetonitrile, 10 mM ammonium acetate, pH 10.2 (100% A to 40% A in 8.5 min). The UHPLC system was coupled online with a Q Exactive system (Thermo, San Jose, CA, USA), scanning in Full MS mode (2 μ scans) at 70,000 resolution in the 60-900 m/z range, 4 kV spray voltage, 15 sheath gas and 5 auxiliary gas, operated in either negative or positive ion mode. Calibration was performed before each analysis using positive or negative ion mode calibration mixes (Piercenet – Thermo Fisher, Rockford, IL, USA) to ensure sub ppm error on the intact mass. Metabolite assignments were performed through the software MAVEN (Princeton, NJ, USA) (1), upon conversion of .raw files into .mzXML format through MassMatrix (Cleveland, OH, USA). The MAVEN software allows for peak picking, feature detection and metabolite assignment using the KEGG pathway database. Assignments were further confirmed by chemical formula determination from isotopic patterns, accurate intact mass, and retention time comparison against an in-house standard library consisting of >700 metabolites from compound classes such as carboxylic acids, amino acids, biogenic amines, polyamines, nucleotides, coenzymes, vitamins, mono- and disaccharides, fatty acids, lipids, steroids, and hormones (Sigma-Aldrich, St. Louis, MO, USA, IROATech, Bolton, MA, USA).

Relative quantitation was performed by exporting integrated peak areas values for statistical analysis including T-Test (significance threshold for *p-values* < 0.05) and principal component analysis/partial least square discriminant analysis (PCA/PLS-DA) and hierarchical clustering analyses, calculated using MultiBase (www.NumericalDynamics.com). Metabolic pathway analysis, PLS-DA and hierarchical clustering was performed using the MetaboAnalyst 3.0 package (www.metaboanalyst.com) (2). Hierarchical clustering analysis (HCA) was also performed through the software GENE-E (Broad Institute, Cambridge, MA, USA). XY graphs were plotted through GraphPad Prism 5.0 (GraphPad Software Inc., La Jolla, CA, USA).

Untargeted Quantitative ¹H-Nuclear Magnetic Resonance Metabolomics Analysis

Ultra-Small Volume Quantitative NMR Spectroscopy: Isolated B-cell progenitors from pooled animals (2 independent experiments; 5 pooled animals/ group; sample size: 8-12 mg) were extracted with 0.2 mL of ice cold methanol/chloroform mixture as previously described (3). The water-soluble fractions were lyophilized overnight and re-dissolved in 30 μ L deuterium oxide (D₂O) with deuterated trimethyl-silyl-propionic acid (d-TMSP, as an external standard). The extracts were transferred into Bruker 1-mm glass capillaries and inserted into the magnet using a 1-mm NMR spinner.

All NMR experiments were performed on a Bruker 500 MHz spectrometer (operating frequency 500.15 MHz) using a Bruker ultra-small volume 1-mm high-resolution inverse TXI (¹H/¹³C/³¹P) Z-gradient microprobe (Bruker BioSpin, Billerica, MA). One dimensional ¹H-NMR spectra were obtained from each sample, with a standard water pre-saturation pulse program “zgpr” (3). The pulse delay of 12.75 s (calculated as 5*T₁) was applied between acquisitions for fully relaxed ¹H-NMR spectra. The external standard TMSP was used as a chemical shift reference (0 ppm).

All spectral acquisition and data analysis were performed using the Bruker TopSpin software. Cell metabolites were identified based on the results from our chemical shift data base and/ or referred to the Human Metabolome Database from the University of Alberta (<http://www.hmdb.ca/>). After performing Fourier transformation, the absolute concentrations of 75 identified endogenous metabolites were then referred to the TMSP integral and calculated as [μ mol/g] according to the equation (4):

$$C_x = \frac{I_x : N_x \cdot C}{I : 9} \cdot V : M_{sample} \quad (2)$$

where C_x = metabolite concentration

I_x = integral of endogenous metabolite ¹H peak

N_x = number of protons in metabolite ^1H peak (from CH, CH₂, CH₃, etc.)

C = TMSP concentration

I = integral of TMSP ^1H peak at 0 ppm (:9 since TMSP has 9 protons)

V = total volume of the sample with D₂O (0.02 mL)

M_{sample} = volume of cell sample (g)

Antibodies:

The following antibodies against mouse antigens were used: phycoerythrin (PE)-conjugated anti-B220 (BD Pharmingen; cat. no. 553090), anti-CD43 (BD Pharmingen, cat. no. 553271), anti-MAC-1 (BD Pharmingen; cat. no. 557397), anti-CD3 (eBioscience; 12-0031-82), anti-CD8 (eBioscience; 12-0081-82), anti-CD4 (eBioscience; 12-0041-83), anti-Ter119 (eBioscience; 12-5921-81), anti-Gr-1 (eBioscience; 12-5931-82); PE-Cy7-conjugated anti-MAC-1 (eBioscience; 25-0012-82); allophycocyanin (APC)-conjugated anti-B220 (eBioscience; 17-0452-82); APCy7-conjugated anti-c-Kit (BD Pharmingen; 553356); FITC-conjugated anti-CD43 (eBioscience; 11-0431-82), anti-Sca-1 (eBioscience; 11-5981-81); and Pacific Blue (e450)-conjugated anti-CD93 (eBioscience; 48-5892-80). Flow cytometry analysis was performed on Cyan, Cytomics FC 500, or Cell Lab Quanta SC (Beckman Coulter) flow cytometers. B-cell progenitors were defined based on their expression of surface markers:

B-progenitors

Pro B-cells: B220^{low}, CD93^{high}, CD43^{high}

Pre B-cells: B220^{low}, CD93^{high}, CD43^{intermediate/low}

Immature B-cells: B220^{high}, CD93^{Negative}, CD43^{Negative}

Stem Cell Populations

LSK: Lin^{Negative}, Sca-1^{Positive}, c-kit^{Positive}, CD150^{Positive}, CD48^{Negative}, CD135^{Negative}

Myeloid Progenitors

Megakaryocyte Erythroid Progenitors: Lin^{Negative}, Sca-1^{Negative}, c-kit^{Positive}, CD34^{Negative}, CD16/32^{Negative}

Common Myeloid Progenitors: Lin^{Negative}, Sca-1^{Negative}, c-kit^{Positive}, CD34^{Positive}, CD16/32^{Negative}

Granulocyte Monocyte Progenitors: Lin^{Negative}, Sca-1^{Negative}, c-kit^{Positive}, CD34^{Positive}, CD16/32^{Positive}

Intracellular staining for phospho-γH2AX: Intracellular cytokine staining was performed as previously described (5). FITC-conjugated anti-phospho-γH2AX (Biolegend; cat. no. 613403) antibody was used to assess diet-induced DNA damage. Stained cells were analyzed on the Cyan ADP Analyzer (Beckman Coulter).

EdU Analysis of progenitor cell populations: EdU analysis of B-cell progenitor cell populations isolated from Balb/c mice maintained on various folate diets were performed using Click-iT EdU Alexa Fluor 647 Imaging Kit (Life Technologies; Ref. No. C10634) as previously described (5). Flow cytometric analysis was used to determine the cell cycle profiles of pro-B, pre-B, and immature B-cell progenitor populations. Samples were run on a Gallios cytometer (Beckman Coulter).

1. Clasquin MF, Melamud E, and Rabinowitz JD. LC-MS data processing with MAVEN: a metabolomic analysis and visualization engine. *Curr Protoc Bioinformatics*. 2012;Chapter 14(Unit14 1.
2. Xia J, Sinelnikov IV, Han B, and Wishart DS. MetaboAnalyst 3.0--making metabolomics more meaningful. *Nucleic Acids Res*. 2015;43(W1):W251-7.
3. Serkova NJ, and Glunde K. Metabolomics of cancer. *Methods Mol Biol*. 2009;520(273-95.
4. Serkova NJ, Jackman M, Brown JL, Liu T, Hirose R, Roberts JP, Maher JJ, and Niemann CU. Metabolic profiling of livers and blood from obese Zucker rats. *Journal of hepatology*. 2006;44(5):956-62.
5. Henry CJ, Casas-Selves M, Kim J, Zaberezhnyy V, Aghili L, Daniel AE, Jimenez L, Azam T, McNamee EN, Clambey ET, et al. Aging-associated inflammation promotes selection for adaptive oncogenic events in B cell progenitors. *The Journal of clinical investigation*. 2015;125(12):4666-80.

Supplemental Figure Legends and Figures

SUPPLEMENTAL FIGURE LEGENDS

Figure S1. Peripheral Leukocyte Numbers in Mice Fed Control, Deficient, and Supra Levels of Dietary Folate

(A-D) Complete blood counts were performed on the peripheral blood collected from BALB/ c mice kept on CD, FD, and SD folate diets for 2, 4, and 6 months. Values represent mean \pm SEM of 5-10 mice/ diet at the various time points (a representative experiment is shown). (E) Mice were maintained on CD, FD, and SD folate diets for 1 year, and their weights were determined. Values represent \pm SEM of 5 mice/ diet. Statistical analysis for each experiment was performed using a one-way ANOVA test followed by Tukey's Post-test.

Figure S2. B-progenitor Profiles of Mice Maintained on Diets with Different Folate Levels

Mice were maintained on CD, FD, and SD folate diets for 4 months and flow cytometry was performed in order to determine the number of pro-B, pre-B, and immature B-progenitor cells. (A) A representative gating strategy for B-progenitor cells is shown. The populations were identified as follows: pro-B-progenitor cells (Mac-1⁻, B220^{lo}, CD43^{hi}); pre-B-progenitor cells (Mac-1⁻, B220^{lo}, CD43^{lo}); and immature B-progenitor cells (Mac-1⁻, B220^{hi}). (B) Using the total bone marrow cellularity for each mouse and the percentage of each population as determined via flow cytometry, the total number of pro-, pre-, and immature B-progenitor cells in the tibias and femurs were determined. Statistical analysis was performed using a one-way ANOVA test followed by Tukey's Post-test, and significance was not achieved for any comparison.

Figure S3. Control, Folate-deficient, and Supra-folate Diets Alter Cellular Homeostasis in Distinctive Ways

(A) BALB/c mice were fed CD, FD, and SD diets for 4 months and ultra-high pressure liquid chromatography combined with mass spectrometry (UHPLC-MS) was used to determine the metabolic profiles of B-progenitor cells, heart, liver, and intestinal tissues. Data from 5 mice/diet are shown. (B) Unsupervised hierarchical clustering results are shown for B-progenitor cells. (C-F) Partial least squares-discriminant analysis (PLS-DA) analysis and Metabolite Set Enrichment Analysis (MSEA) were performed to identify metabolic pathways that were significantly enriched in tissue from mice on all diets. PLS-DA and heat maps of the top metabolic pathways that discriminate between the various cells and tissues isolated from the mice described in A are shown. PLS-DA, the standard of multivariate analyses of biological metabolomics data, is a supervised version of unsupervised Principal Component Analysis. In PLS-DA, samples are clustered around arbitrary axes, defined as principal components (PC) that explain a given percentage of the variance (eigenvalues) for metabolite measurements across samples.

Figure S4. Control, Folate-deficient, and Supra-folate Diets Alter Cellular Metabolism in B-progenitor Cells

BALB/c mice were fed CD, FD, and SD diets for 4 months and UPHLC-MS was used to determine the metabolic profiles of B-progenitor cells. **(A)** A heatmap of the amino acids that discriminate between B-progenitor cells isolated from mice on these diets is shown (**data are from Table S2**). **(B and C)** Significantly altered metabolic pathways and metabolic function (alteration in enzymatic activity) in B-progenitor cells determined using MSEA.

Figure S5. Folate Deficiency and Excessive Levels of Folic Acid Reduce Glutathione Levels in B-progenitor Cells

(A and B) BALB/c mice were fed CD, FD, and SD diets for 4 months and specific metabolites involved in glutathione production were identified in B-progenitor cells using UHPLC-MS (data are from Table S2). Values represent mean \pm SEM of 5 mice/ diet. A one-way ANOVA followed by a Tukey's Post-test was used to compare the effects of all diets to each other.

Figure S6. Altering Dietary Folate Levels and Anti-Folate Drugs Induce Defective Pyrimidine Synthesis in B-progenitor Cells

BALB/c mice were fed CD, FD, and SD diets for 4 months or treated with MTX (**as described in Figures 3 and 5 respectively**) and specific metabolites in the pyrimidine nucleotide synthesis pathway that were altered by changes in dietary folate levels were identified in B-progenitor cells using UPHLC-MS. Values represent mean \pm SEM of 5 mice/ diet and \pm SEM of 4 mice/ PBS or MTX treatment. A one-way ANOVA followed by a Tukey's Post-test was used to compare the effects of all diets to each other, and a Student's t-test was used to compare the effects of PBS and MTX treated mice.

Figure S7. Modulating Dietary Folate Levels Does not Significantly Alter the Representation of Long-term Hematopoietic Stem and Myeloid Progenitor Cells in the Bone Marrow

BALB/c mice were fed CD, FD, and SD diets for 2 months and the representation of bone marrow derived, long-term hematopoietic stem and progenitor cells (LT-HSC) **(A-C)** and myeloid progenitors (CMP and total Mac-1⁺ cells) **(D-F)** were determined by flow cytometric analysis. The number of LT-HSC and myeloid progenitor cells in the tibias and femurs was calculated using the total bone marrow cellularity for each mouse and the percentage of each population as determined via flow cytometric analysis. A one-way ANOVA followed by a Tukey's Post-test was used to compare the effects of all diets to each other.

Table S1. Nuclear Magnetic Resonance Analysis of B-progenitor Cells Isolated from Mice Maintained on Control, Folate-deficient, and Supra-folate Diets for Four Months.

Table S2. Ultra-high Pressure Liquid Chromatography-Mass Spectrometry (UHPLC-MS) Analysis of Various Tissues Isolated from Mice Maintained on Control, Folate-deficient, and Supra-folate Diets for Four Months.

Table S3. Metabolite Set Enrichment Analysis (MSEA) of Various Tissues Isolated from Mice Maintained on Control, Folate-deficient, and Supra-folate Diets for Four Months.

Table S4. Ultra-high Pressure Liquid Chromatography-Mass Spectrometry (UHPLC-MS) Analysis of B-progenitor Cells Isolated from Mice treated with PBS or Methotrexate (MTX) for Five Consecutive Days.

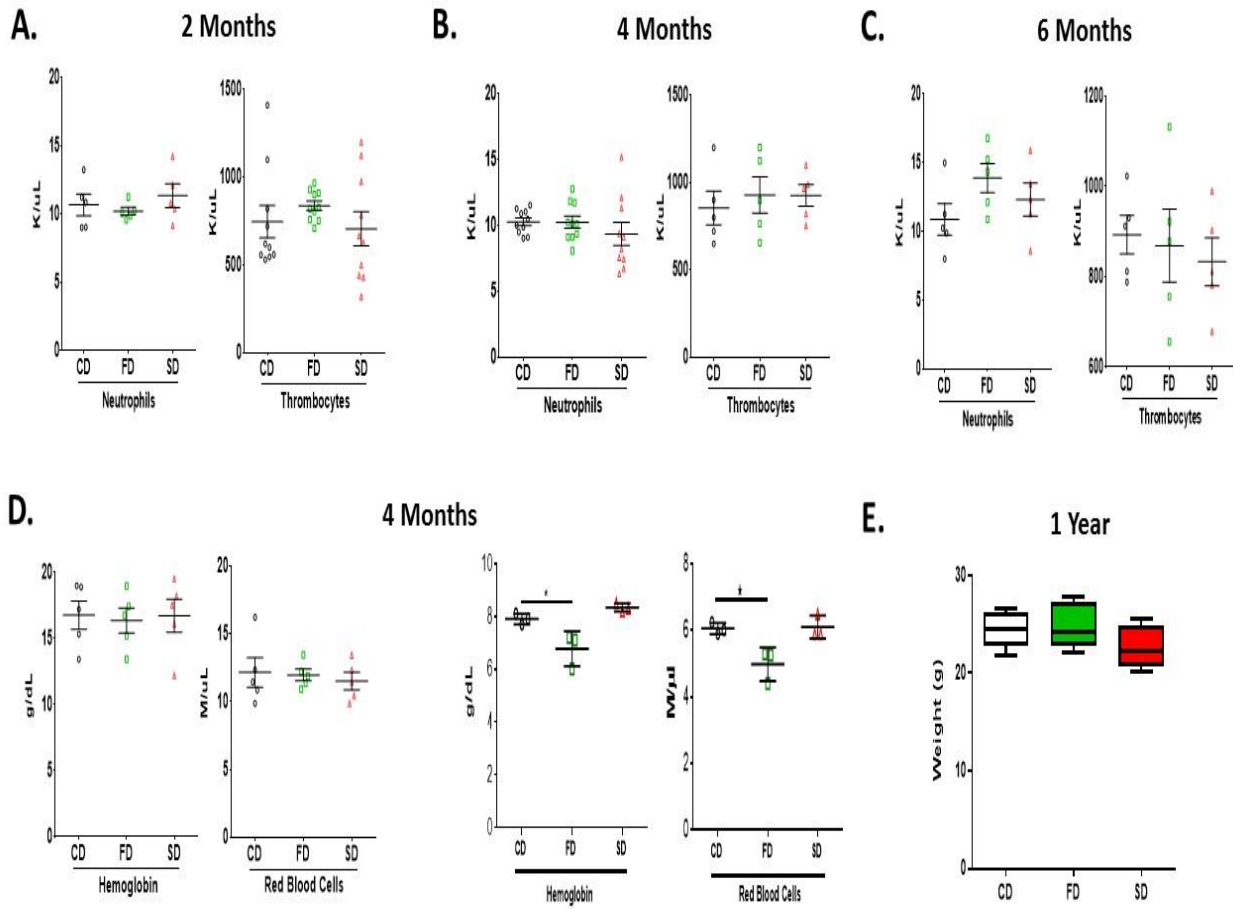


Fig. S1

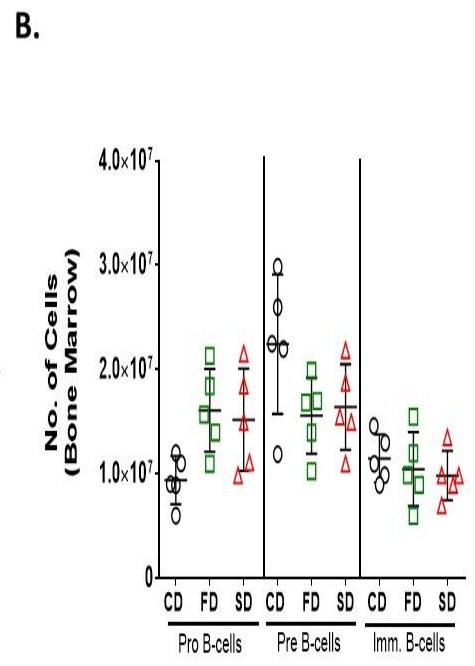
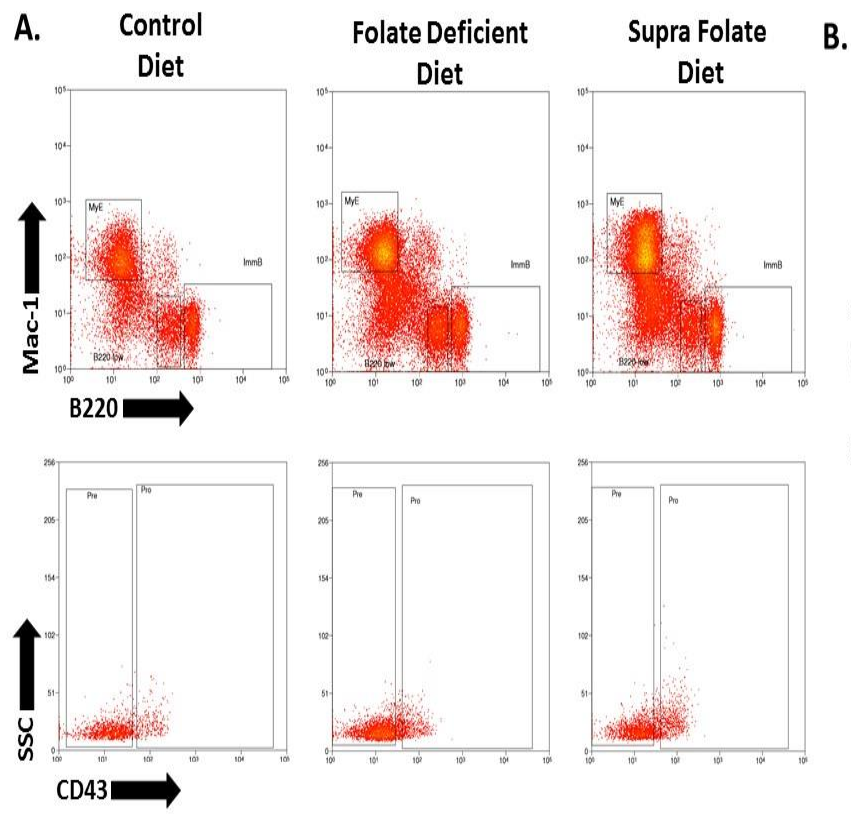


Fig. S2

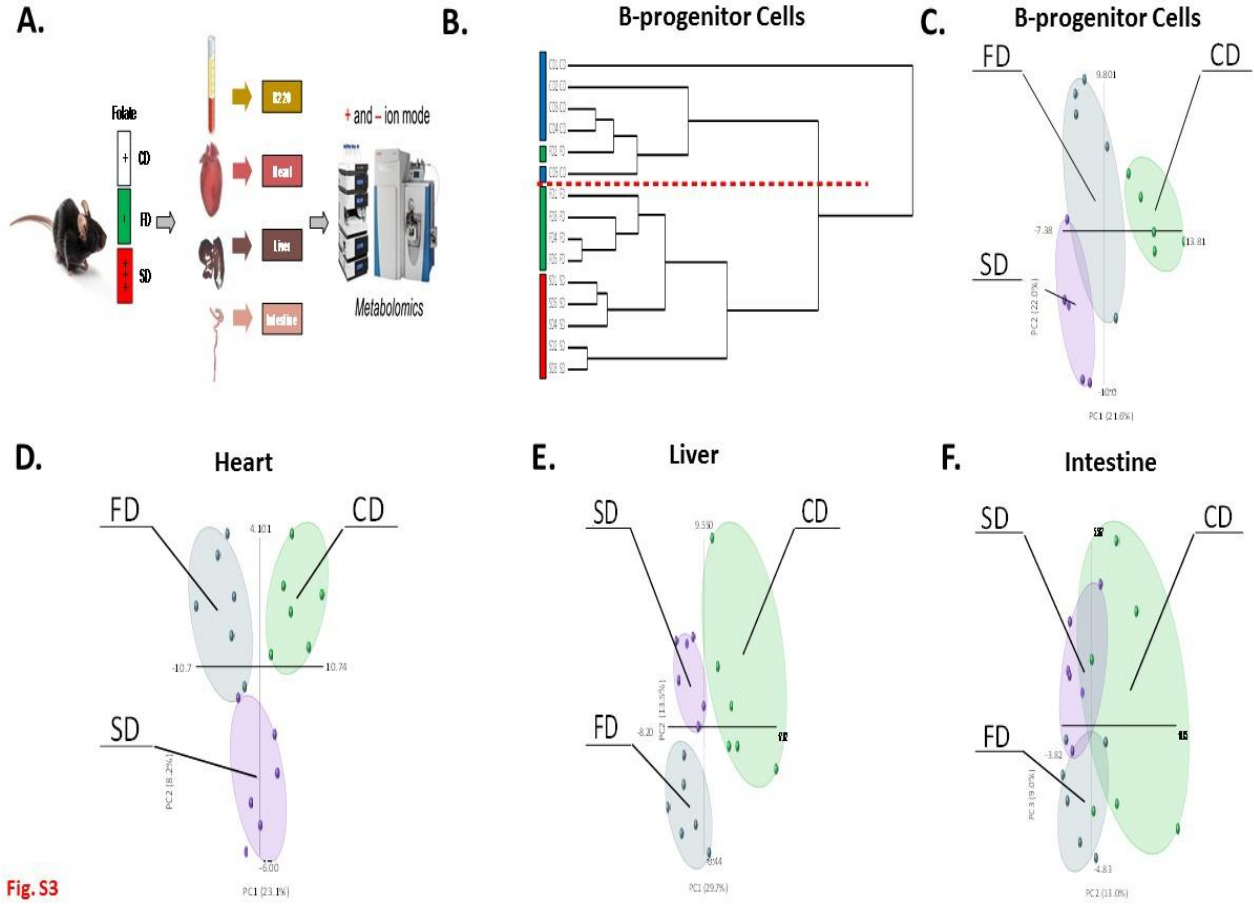
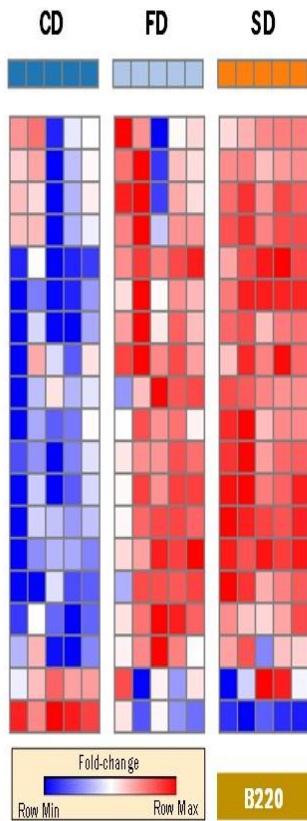
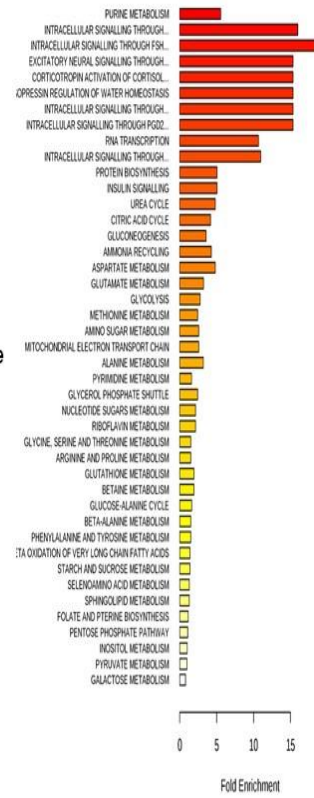


Fig. S3

A. Amino Acid Changes in B-progenitors



B. Metabolic Sets Enrichment Overview (B-progenitors)



C. Enrichment Overview (B-progenitors)

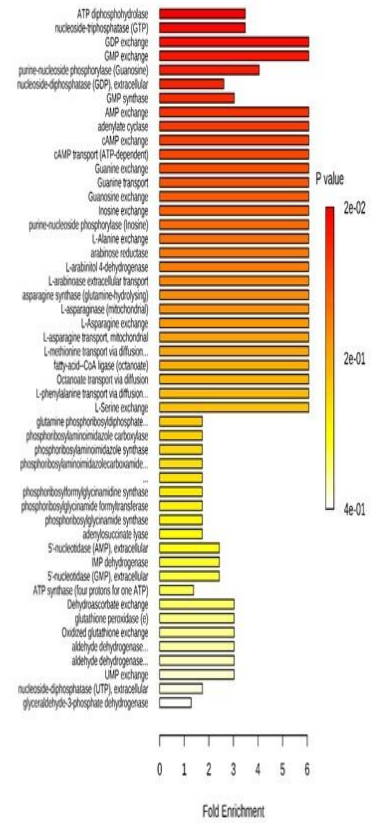


Fig. S4

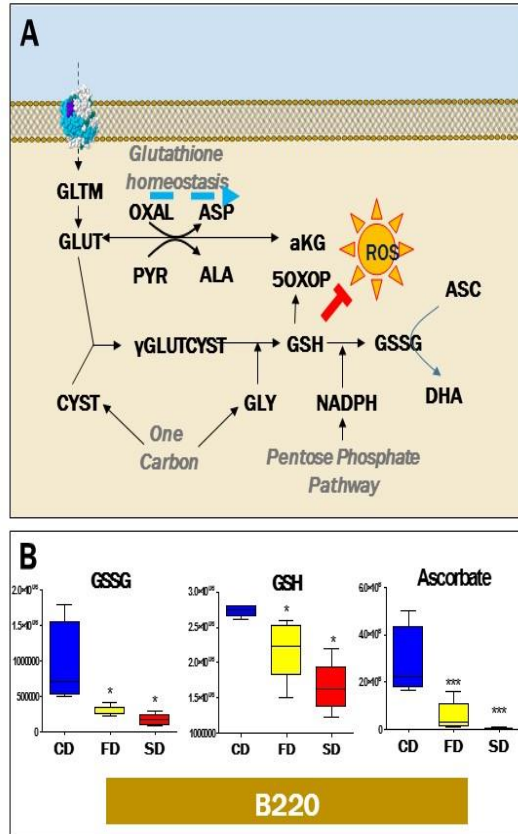


Fig. S5

Pyrimidine biosynthesis

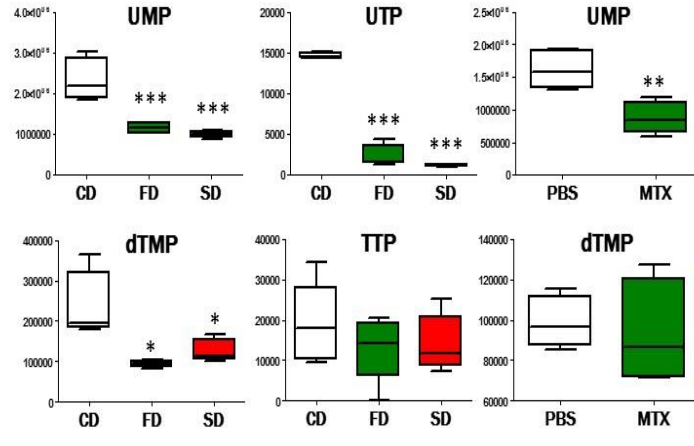
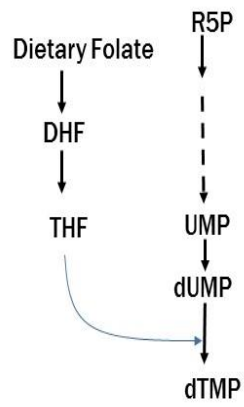


Fig. S6

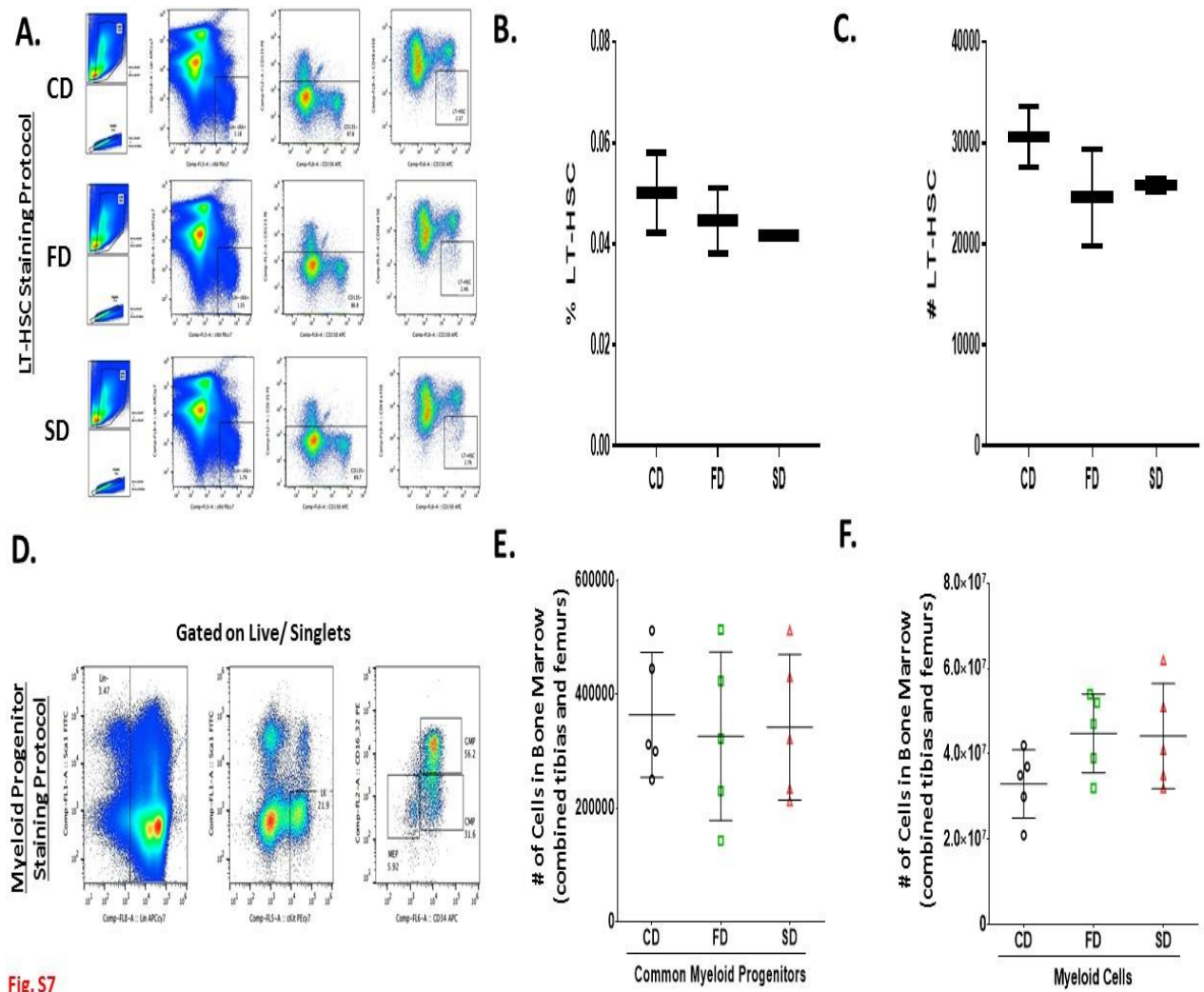


Fig. S7